Sendai Virus-Erythrocyte Membrane Interaction: Quantitative and Kinetic Analysis of Viral Binding, Dissociation, and Fusion

DICK HOEKSTRA* AND KARIN KLAPPE

Laboratory of Physiological Chemistry, University of Groningen, 9712 KZ Groningen, The Netherlands

A kinetic and quantitative analysis of the binding and fusion of Sendai virus with erythrocyte membranes was performed by using a membrane fusion assay based on the relief of fluorescence self-quenching. At 37°C, the process of virus association displayed a half time of 2.5 min; at 4°C, the half time was 3.0 min. The fraction of the viral dose which became cell associated was independent of the incubation temperature and increased with increasing target membrane concentration. On the average, one erythrocyte ghost can accommodate ca. 1,200 Sendai virus particles. The stability of viral attachment was sensitive to a shift in temperature: a fraction of the virions (ca. 30%), attached at 4°C, rapidly (half time, ca. 2.5 min) eluted from the cell surface at 37°C, irrespective of the presence of free virus in the medium. The elution can be attributed to a spontaneous, temperature-induced release, rather than to viral neuraminidase activity. Competition experiments with nonlabeled virus revealed that viruses destined to fuse do not exchange with free particles in the medium but rather bind in a rapid and irreversible manner. The fusion rate of Sendai virus was affected by the density of the virus particles on the cell surface and became restrained when more than 170 virus particles were attached per ghost. In principle, all virus particles added displayed fusion activity. However, at high virus-to-ghost ratios, only a fraction actually fused, indicating that a limited number of fusion sites exist on the erythrocyte membrane. We estimate that ca. 180 virus particles maximally can fuse with one erythrocyte ghost.

Sendai virus is a membrane-bounded virus which belongs to the paramyxovirus family. The virus possesses membrane fusion activity which is imperative for its survival, as this property enables the virion to introduce its genome into the cytoplasm of the host cell for replication. Passage of the genome across the plasma membrane results from a fusion process between the viral envelope and the cell surface at neutral pH (2, 17, 29, 36). The fusion process is a two-step reaction, involving a binding step and the actual fusion event, and is mediated by the viral spike glycoproteins HN and F (4). Cell attachment is accomplished by an interaction between HN and sialic acid-containing glycoproteins (32, 39) or glycolipids (14, 34), and the F protein, which consists of two disulfide-bonded polypeptides, F_1 and F_2 (4), has been identified as the fusion factor. It has been proposed that a hydrophobic segment contained in the F_1 polypeptide of this protein (7, 15) interacts directly with the target membrane (15, 30, 36), causing a (local) perturbation of the bilayer structure which subsequently leads to bilayer merging.

Various techniques have been used to assess viral fusion activity and to investigate the underlying mechanism. Some of the procedures focus on events secondary to the actual fusion reaction (e.g., hemolysis and cell fusion), whereas other methods either do not provide (8, 26, 33) or provide only after tedious labor (9, 19) an accurate, quantitative insight into the kinetics or extent of fusion. For a proper interpretation of the mechanism of viral fusion activity, the acquirement of such data seems imperative (36, 37).

Recently, we developed a membrane fusion assay, based on the relief of fluorescence self-quenching, which can serve as an excellent tool for the direct study of questions related to quantitative and kinetic aspects of virus-host cell interaction (11). Fusion between virus particles and the target membrane can be monitored continuously without the need to separate fused and nonfused particles. In addition, the

fraction of the cell-associated virus which fuses or binds to the cell surface can readily be determined. The aim of the present work was to obtain a detailed view of the interaction events between Sendai virus and erythrocyte membranes in terms of the kinetics and extent of viral attachment, detachment, and fusion. In addition, we analyzed the influence of a variety of incubation conditions as well as the effect of the reducing agent dithiothreitol (DTT) on the capacity of the virions to bind and fuse with erythrocyte membranes.

MATERIALS AND METHODS

Virus. Sendai virus (Z strain) was grown in the allantoic cavity of 10-day-old embryonated chicken eggs. Allantoic fluid was harvested after 72 h, and cellular debris was removed by centrifugation at 5,000 × g (30 min, 4°C). The virus was purified by differential centrifugation (20), washed twice with phosphate-buffered saline, and stored at −70°C. The stocks used throughout the fusion experiments contained ca. 350 hemagglutinating units per ml of allantoic fluid and had an infectivity titer of ≥10^{10} PFU/ml. Therefore, they can be defined as standard preparations of Sendai virus without defective interfering particles (31). Unless indicated otherwise, the amount of virus given in the text refers to the amount of viral protein.

We occasionally expressed the amount of virus in terms of the number of virus particles. This number was calculated based on the assumption that (i) Sendai virus contains 276 nmol of phospholipid per mg of protein (18), and the average diameter of the particles is 150 nm (17), whereas the surface area of a phospholipid molecule is 7 nm^2, or (ii) the molecular weight of the virus is 5 × 10^8 (37), and 70% by weight is protein (16). Thus, an average of 1.3 × 10^9 virus particles per µg of virus protein was calculated.

Preparation of R_{18}-labeled virus. Fluorescently tagged Sendai virus was prepared as described in detail elsewhere (11, 12). Briefly, the virus (approximately 1 mg of protein) was suspended in 1 ml of 120 mM KCl–30 mM NaCl–10 mM

* Corresponding author.

sodium phosphate buffer (pH 7.4; KNP buffer). An ethanolic solution (≤ 10 μl) of octadecyl rhodamine B chloride (R_{18}; Molecular Probes Inc., Junction City, Oreg.) was injected into the mixture, under vigorous vortexing, with a Hamilton syringe (final R_{18} concentration, 15 μM). After incubation for 1 h at room temperature, noninserted probe was removed by gel filtration on Sephadex G-75. The membrane-labeled virus was recovered in the void volume fraction, the amount of virus was determined by protein measurement, and the preparation was stored on ice.

Erythrocyte ghosts. Sealed erythrocyte ghosts were prepared by hypotonic hemolysis of human erythrocytes (type A^+) in 5 mM sodium phosphate buffer (pH 8.0; 13). Prior to resealing, the ghosts were loaded with albumin (5% [wt/vol]) immediately after lysis by a brief incubation on ice (15 min). After resealing, at 37°C (45 min) in the presence of 1 mM Mg^{2+}, the ghosts were washed thrice with KNP buffer, and the final pellet was resuspended in the same buffer; the suspension was stored on ice. The amount of ghosts was expressed as micrograms of protein, which was determined by measuring protein (before the addition of albumin) and occasionally verified by determining lipid phosphorus after lipid extraction. The amount of protein was then calculated, assuming that 674 nmol of phospholipid corresponds with 1 mg of protein (5). When the amount of ghosts is expressed as the number of cells, we assumed that 1 mg of protein equals 1.8×10^9 cells.

Fusion measurements. Under the conditions of viral membrane labeling described above, the fluorescent dye R_{18} is inserted into the membrane at a surface density that causes self-quenching of fluorescence. Upon fusion between the viral membranes and the nonlabeled target membranes (erythrocyte ghosts), relief of self-quenching occurs, resulting in a proportional increase in fluorescence intensity. The increase in fluorescence, as a direct measure of fusion, can be monitored continuously in a fluorometer. A detailed account of this assay has been presented elsewhere (11, 12).

The fusion experiments described in this work were performed as follows. R_{18}-labeled virus was suspended in a cuvette containing KNP buffer (pH 7.4) at 37°C. Subsequently, ghosts were added, and the development of R_{18} fluorescence (excitation wavelength, 560 nm; emission wavelength, 590 nm; slit width, 4.5 nm) was monitored continuously with a Perkin-Elmer MPF 43 spectrophotofluorometer equipped with a chart recorder. The temperature was controlled with a thermostatted circulating water bath. In some experiments the virus was allowed to attach to the ghost membrane, before fusion, by incubation on ice for 15 min in a small volume of KNP buffer. Prewarmed buffer was then added, and the mixture was rapidly transferred to a cuvette which was then placed in the fluorometer for the monitoring of fusion at 37°C, as described above. The final incubation volume in all fusion experiments was 2 ml. For calibration of the fluorescence scale, the initial residual fluorescence of the R_{18}-labeled virus was taken as the zero level, and the fluorescence at infinite probe dilution was taken as 100%. The latter value was obtained by determining the level of fluorescence after the addition of Triton X-100 (1% [vol/vol]), corrected for sample dilution. The results are expressed as the percentage of fluorescence that would be obtained upon infinite dilution. In the case of Sendai virus-ghost fusion, the percentage of R_{18} fluorescence is directly proportional to the extent of fusion (11). The initial fusion rates were determined from the slope of the steepest part of the fluorescence tracings (percentage of R_{18} fluorescence per minute). The final extent of

fusion was assessed by reading the R_{18} fluorescence after incubation of virus with ghosts for 20 to 24 h at 37°C. Finally, the fraction of virus which fused, relative to the total fraction of cell-associated virus (after the removal of nonbound virus), was calculated from the extent of R_{18} fluorescence increase, measured before and after the addition of Triton X-100, relative to the same ratio obtained for nonfused virus.

Virus-binding assay. R_{18}-labeled Sendai virus was incubated with ghosts in an appropriate volume (see figure legends) of KNP buffer for 15 min on ice. Nonbound virus was removed by centrifugation in an Eppendorf table centrifuge (4 min, 10,000 $\times$ g, 4°C), and the cells were washed with ice-cold buffer. After the addition of Triton X-100 (1% [vol/vol]), the R_{18} fluorescence was measured in the pellet and the combined supernatant fractions to determine the fraction of bound (cell associated) and nonbound virus, respectively. To eliminate the possibility of cosedimentation of aggregated virus particles, the virus preparation was centrifuged under conditions similar to those described above, before incubation with ghosts.

Virus-induced hemolysis. Sendai virus was incubated with human erythrocytes (type A^+) for various times. After the removal of intact cells, the percentage of hemoglobin release in the supernatant was measured by determining the A_{540} relative to the absorbance assessed after the cells were lysed in the presence of ammonia.

Treatment of the virus with DTT. Double the amount of virus used in the fusion experiments was incubated with the desired concentration of DTT at 37°C for 15 min. The incubation medium consisted of KNP buffer (pH 7.4); the final volume was 150 μl. A 75-μl sample was taken and injected into the fusion medium. Fusion was initiated by the addition of ghosts.

RESULTS

Virus binding kinetics. The time course of Sendai virus attachment to erythrocyte membranes is shown in Fig. 1. At 37°C the initial binding kinetics was slightly faster than that observed at 4°C as reflected by half times of approximately 2.5 and 3.0 min, respectively. At either temperature, 50 to 55% of the viral dose added became cell associated eventually, indicating a relatively temperature-independent mode of virus binding. As anticipated (12), only at 37°C was a steady decrease in fluorescence quenching observed, resulting from membrane fusion and subsequent randomization of viral and erythrocyte membrane components (see below).

When nonbound virions were removed after incubation at either 37 or 4°C for 15 min, followed by the resuspension of the cells in medium of the same temperature as that during preincubation, less than 5% of the cell-associated virus eluted from the ghost membrane during an additional incubation of at least 30 min. Hence, an apparent irreversible binding was established under both conditions. However, substantial release of virus was observed when the temperature of the cell suspension, pretreated with viruses at 4°C, was elevated to 37°C (see below).

Parameters affecting the extent of virus binding. At a fixed ratio of virus over ghosts (25 μg of viral protein per 50 μg of ghost protein), the final incubation volume (0.1 to 1.5 ml) slightly affected the amount of virus that bound to the erythrocyte membrane after 15 min of incubation at 4°C (data not shown). Thus, relative to the extent of binding obtained at a final incubation volume of 0.1 ml, the total cell-associated virus fraction decreased by approximately 10% when the incubation volume was 1.0 ml and by approximately 20% at a final volume of 1.5 ml. A similar incubation
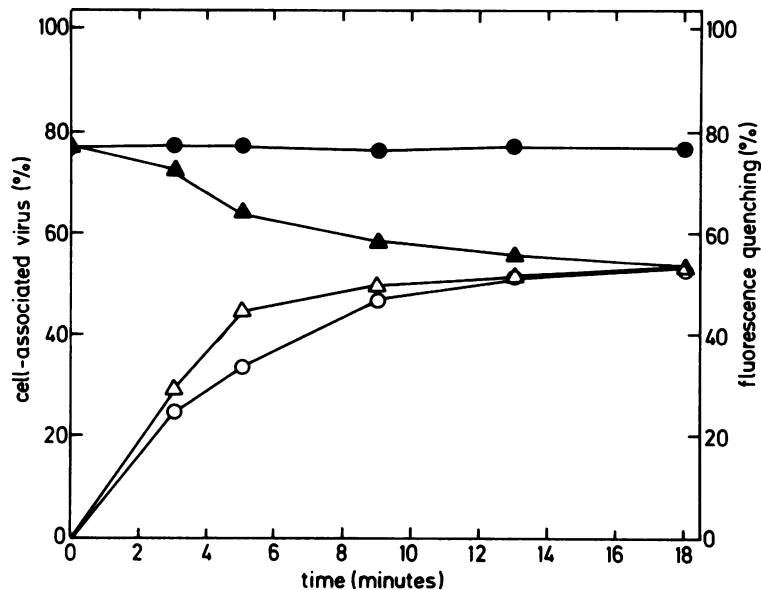
FIG. 1. Kinetics of Sendai virus binding to erythrocyte ghost membranes. R_{18}-labeled virus (30 µg of protein) was incubated with erythrocyte ghosts (100 µg of protein) in a final volume of 0.4 ml at 4 or 37°C for various times. Nonbound virus was then removed by centrifugation. The ghost pellet was resuspended, transferred to a new tube, and washed once. The cell-associated virus fraction (O, 4°C; △, 37°C) was determined by measuring fluorescence in the cell pellet and supernatant fractions after the addition of Triton X-100 (1% [vol/vol]) as described in Materials and Methods. The percentage of fluorescence quenching (●, 4°C; ▲, 37°C), indicating the extent of lipid dilution, was determined from the ratio of fluorescence measured before and after the addition of detergent. Note that the percent fluorescence quenching represents the actual quenching obtained for a virus preparation labeled as described in Materials and Methods.

volume-dependent decrease in viral attachment was obtained at 37°C.

Virus binding to erythrocyte membranes is shown in Fig. 2 as a function of virus and ghost concentration. The extent of virus binding increased with increasing ghost concentration (△). At a fixed concentration of erythrocyte ghosts (50 µg of protein per 0.5 ml), the fractional virus binding (O), i.e., the fraction of the total virus dose added, varied proportionally with the virus concentration, provided that the virus concentration was below 50 µg of protein per 0.5 ml. At higher virus concentrations, the fractional binding leveled off, displaying a tendency to saturate. To estimate the number of virus particles which can maximally bind to the erythrocyte ghost membrane, the attached multiplicity (micrograms of virus bound per microgram of ghosts) was plotted versus the amount of virus added (●; 6, 40). The number of particles attached was then calculated from the plateau of the plots. With four different batches of virus and erythrocyte ghosts, the values attained at saturation varied between 1 and 2.5 µg of virus protein attached per µg of ghost protein. This corresponds to ca. 700 to 1,750 virus particles per ghost, assuming that 1 µg of virus protein contains 1.3×10^9 virus particles, whereas 1 µg of ghost protein equals 1.8×10^6 cells (see Materials and Methods).

Stability of virus binding. To determine the potential reversibility of virus attachment, viruses (260 µg of protein) were allowed to bind to the ghost membranes (750 µg) during 15 min at 4°C in a final incubation volume of 3 ml. Subsequently, nonbound and loosely bound virions were removed, and the ghost suspension was divided into two equal fractions. One fraction was further incubated at 4°C, and the other was incubated at 37°C. At various times, samples were withdrawn, and the dissociation of cell-associated virus was determined. At 4°C approximately 5% of the initially bound virus fraction dissociated from the target membrane within 2
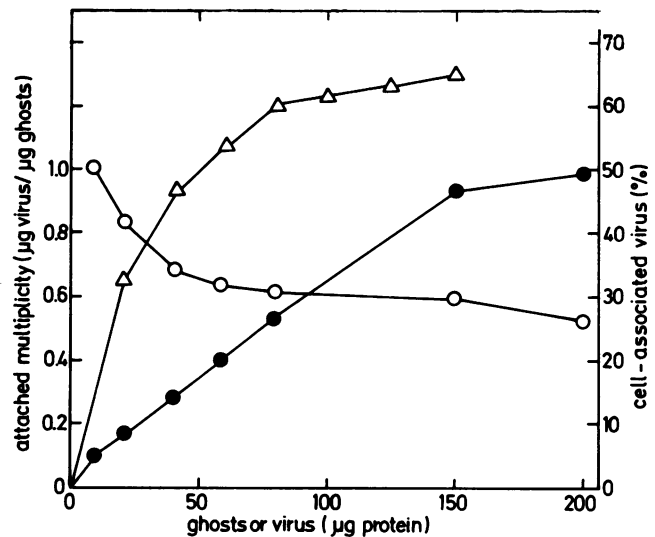

FIG. 2. Binding of virus to erythrocyte membranes as a function of virus and ghost concentration. Ghosts (50 µg of protein) were incubated with increasing amounts of Sendai virus for 15 min at 4°C. The final incubation volume was 0.5 ml. Nonbound virus was removed as described in the legend to Fig. 1, and binding (O), determined by measuring fluorescence in the pellets and supernatants after the addition of Triton X-100, was plotted as a function of the amount of virus. To determine the maximal binding capacity, the extent of binding was recalculated to the amount (in micrograms) of virus versus ghost protein (attached multiplicity) and plotted as a function of the amount of virus added (●). Binding of the virus as a function of ghost concentration was determined similarly, except that R_{18}-labeled Sendai virus (25 µg) was incubated with various amounts of ghosts (△) for 15 min at 4°C in a final volume of 0.25 ml.

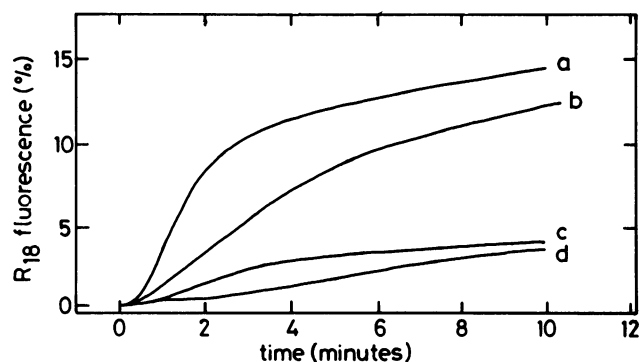FIG. 3. Effect of a low-temperature preincubation on the fusion kinetics of Sendai virus. R_{18}-labeled Sendai virus (15 μg) was incubated with ghosts at 4°C for 15 min (a and c), prior to incubation at 37°C, or was directly added to the ghosts at 37°C (b and d). The kinetics of fusion were monitored continuously, as described in Materials and Methods. The amounts of ghosts were 130 (a and b) and 30 (c and d) μg of protein.

min after the ghost-virus complex was resuspended. At 37°C, a larger fraction was eluted with a half time of approximately 2.5 min and a maximal release of approximately 30%, reached after 10 min. The most obvious explanation for the observed release of virus is the cleavage of the virus from its receptor, mediated by viral neuraminidase activity, which is associated with the HN protein (4). To test this possibility, the experiment was repeated in the presence of a neuraminidase inhibitor, 2-deoxy-2,3-dehydro-N-acetylneuraminic acid (23, 35). It turned out, however, that the release at 4°C remained unaltered in the presence of the inhibitor, whereas at 37°C release was only minimally affected, i.e., 25% still readily dissociated from the cell surface, indicating that virus release cannot be attributed to viral neuraminidase activity. The major fraction, approximately 70% of the initial cell-associated virus fraction, remained firmly attached to the ghost surface and may subsequently become prone to fuse with the erythrocyte membrane.

Effect of preattachment on virus-ghost fusion. As demonstrated elsewhere (12), hemolysis or fusion takes place at 37°C irrespective of preincubation of the virus with the target membrane at 4°C. Because the binding kinetics are different, i.e., after 15 min of incubation at 4°C, the membrane surface is covered with attached virus (Fig. 1), a difference in the initial fusion kinetics is expected. This indeed appeared to be the case (Fig. 3). As a function of ghost concentration, prior attachment resulted in a 1.5- to 2-fold increase in the initial fusion rate (Fig. 4A). The final extents of fusion, as estimated after 20 h, were essentially the same, i.e., independent of whether viral preattachment had taken place (see below). Because the final fluorescence levels tend to saturate at high ghost concentrations (Fig. 4A), the results suggest that the fusion capacity of the ghost membrane for the virus is finite. The maximal fusion capacity was determined by plotting the input multiplicity versus the number of fused virus particles (Fig. 4B). From the reciprocal of this plot (insert), it was calculated that a maximum of approximately 180 virus particles can fuse per erythrocyte ghost.

Binding versus fusion. To examine more closely the fate of the virus particles with respect to binding and fusion at 37°C, various amounts of erythrocyte ghosts were incubated with a fixed amount of virus for 15 min. After the removal of nonbound virions, the cell-associated virus fraction (O) and
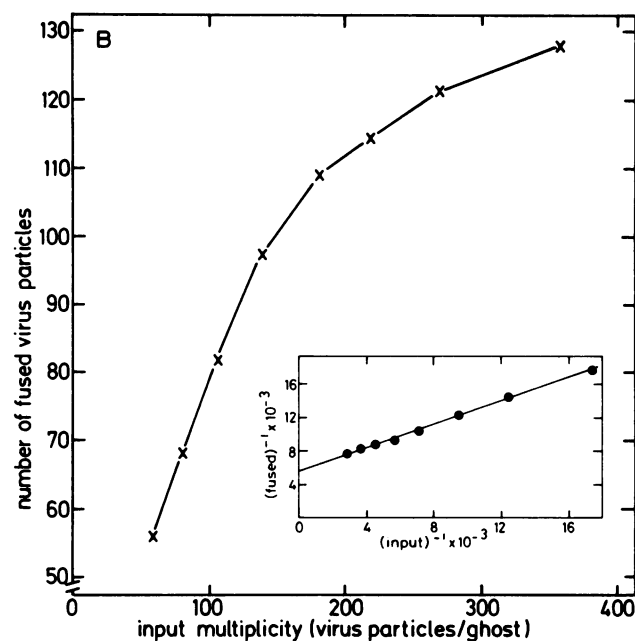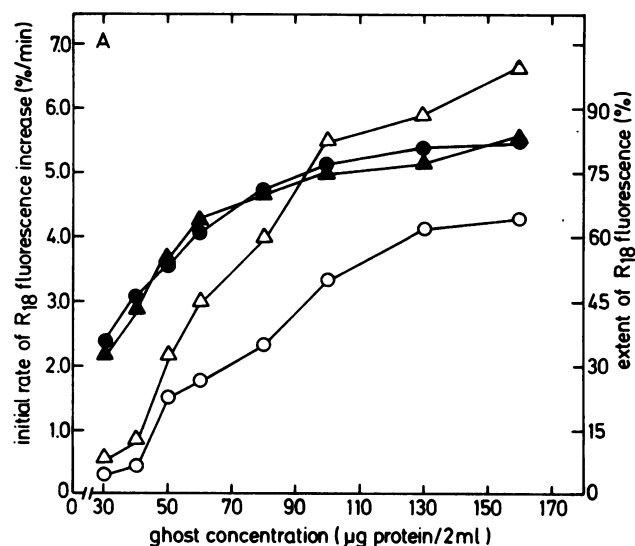

FIG. 4. (A) Effect of preattachment of the virus to the target membrane on the initial rate and final extent of fusion as a function of the target membrane concentration. R_{18}-labeled virus (15 μg) was incubated with various amounts of ghosts at 4°C in a final volume of 1 ml. After 15 min, prewarmed buffer was added to raise the incubation temperature to 37°C and the final volume to 2 ml. Alternatively, the same amount of virus was added directly to the cell suspension at 37°C. The kinetics of fusion were then monitored continuously in a fluorometer, and the initial fusion rate was determined. The incubation mixtures were then left for 24 h, after which the final extent of fusion was determined by measuring fluorescence before and after the addition of Triton X-100. Symbols: △ and ▲, initial rate and final extent of fusion, respectively, after preincubation at 4°C; O and ●, rate and extent of fusion, respectively, when the virus was directly added at 37°C. (B) Determination of the maximal fusion capacity per ghost. The extent of fusion (see panel A) was recalculated as the number of virus particles fused after 24 h and plotted as a function of the number of virus particles added per ghost. For calculations we assumed that 1 μg of virus protein equals 1.3×10^9 virus particles and that 1 μg of ghost protein corresponds to 1.8×10^6 cells. The insert shows the reciprocal plot.
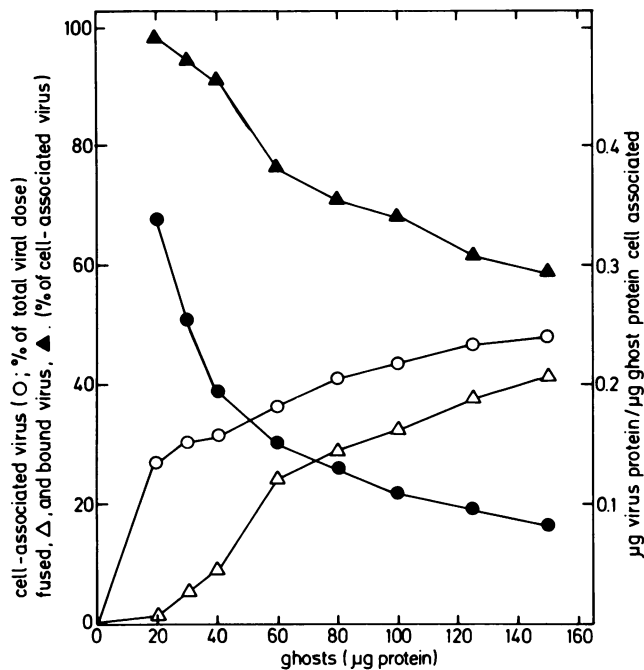
FIG. 5. Determination of the extent of fusion and binding of Sendai virus as a function of the target membrane concentration. R_{18}-labeled virus (25 μg of protein) was incubated with various amounts of erythrocyte ghosts in a final volume of 0.25 ml for 15 min at 37°C. Nonbound virus was removed, and the cells were washed once. The fraction of the total viral dose that became cell associated was determined by measuring fluorescence in the cell pellet and supernatant after the addition of Triton X-100 (O). The fraction of the cell-associated virus fraction that fused during the 15-min incubation period was determined by measuring the cell-associated fluorescence before and after the addition of Triton X-100 (△), and the fraction of bound virus (▲) was deduced from the extent of fusion. The ratio of micrograms of virus protein bound per microgram of ghost protein (●) was obtained by converting the percentage of cell-associated virus to the amount of attached viral protein.
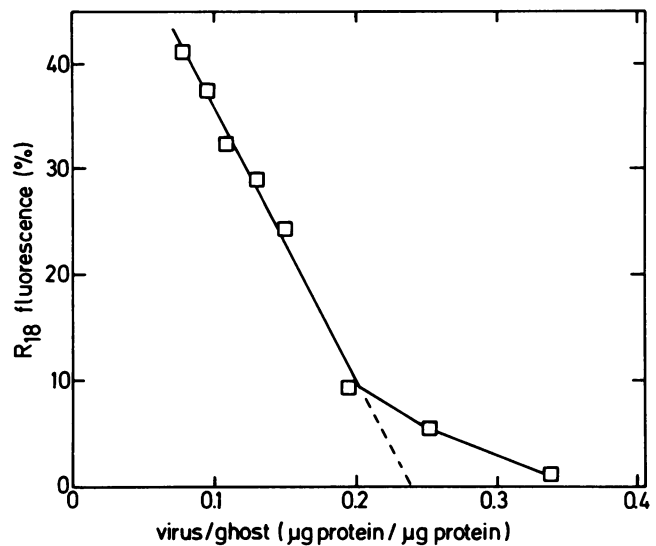

FIG. 6. Relationship between viral fusion activity and the number of virus particles per ghost. The data were taken from the experiment described in Fig. 5. The extent of fusion reached after 15 min at 37°C, as revealed by relief of fluorescence quenching, was plotted as a function of the amount of viral protein associated per microgram of ghost protein after that time.

the extent of this fraction that had fused with the target membrane (△) were determined (Fig. 5). In addition, the ratio of the amount of virus per microgram of ghosts was calculated and plotted (●) as a function of ghost concentration. Consistent with the results obtained for binding per se (at 4°C; Fig. 2), the fraction of virus particles that became cell associated at 37°C increased with increasing ghost concentration. Furthermore, the number of virus particles per ghost (●) decreased hyperbolically, very similar to the case with binding at 4°C. The sigmoidlike plot of the extent of fusion reached after 15 min versus ghost concentration (△) suggests that fusion was inhibited under conditions in which a relatively large amount of virus was attached to the membrane surface, i.e., at a relatively high virus-to-ghost ratio, at the onset of the incubation. This is more clearly revealed when the extent of fusion versus the ratio of (cell-associated) virus over ghosts is plotted. When the amount of ghost-associated virus particles was less than approximately 0.24 μg of viral protein per μg of ghost protein, the extent of fusion increases linearly (Fig. 6). At higher ratios, the fusion capacity deviates from linearity and becomes relatively restrained. This suggests that when the cells are densely populated with attached virus particles adjacent particles affect one another such that fusion becomes impaired.

As described above, part of the cell-associated virus fraction was released into the medium when, after preincubation at 4°C, the temperature was raised to 37°C. Of the remaining cell-bound fraction, a portion fused with the membrane, whereas the residual part was identified at the cell surface as intact virus particles, still present after 15 min of incubation (Fig. 5). These observations evoked two questions. First, are all virus particles which are attached to the membranes after the removal of nonbound viruses eventually prone to fusion, and, second, what is the fate of the virus particles which do not become cell associated after preincubation at 4°C when left in the incubation medium upon raising the temperature to 37°C? To examine the first question, R_{18}-labeled virus was incubated with various amounts of erythrocyte ghosts for 15 min at 4°C. Nonbound virus was subsequently removed, and the cells were transferred to 37°C. After various times, up to 20 h, samples were taken, and the extent of fusion, as revealed by an increase in R_{18} fluorescence, was determined. The fusion reaction displayed a half time of ca. 9 min and was more than 90% complete after 4 h (Fig. 7A). Under none of these conditions did the final level of fusion reach 100%, even after an incubation period as long as 20 h. The fate of the nonfused particles was analyzed in more detail in the case of the incubation in which the virus was initially added to 100 μg of ghosts. After the low-temperature preincubation, time zero in Fig. 7A, 57% of the viral dose added was cell associated. Within minutes after the initiation of fusion at 37°C, part of the cell-associated virus fraction (approximately 30%) eluted from the cell surface (Fig. 7B; ▲). The remaining cell-bound virus fraction was constant during incubation of at least 4 h. These results imply that the fraction of fused virus is underestimated as a result of this release. When viral elution is taken into account, it can be calculated that more than 80% of the truly cell-associated virus had actually fused after 4 h.

When nonadhered virions were left in the medium after preincubation at 4°C, a fraction of the cell-associated virions still dissociated from the cell surface, very similar to that
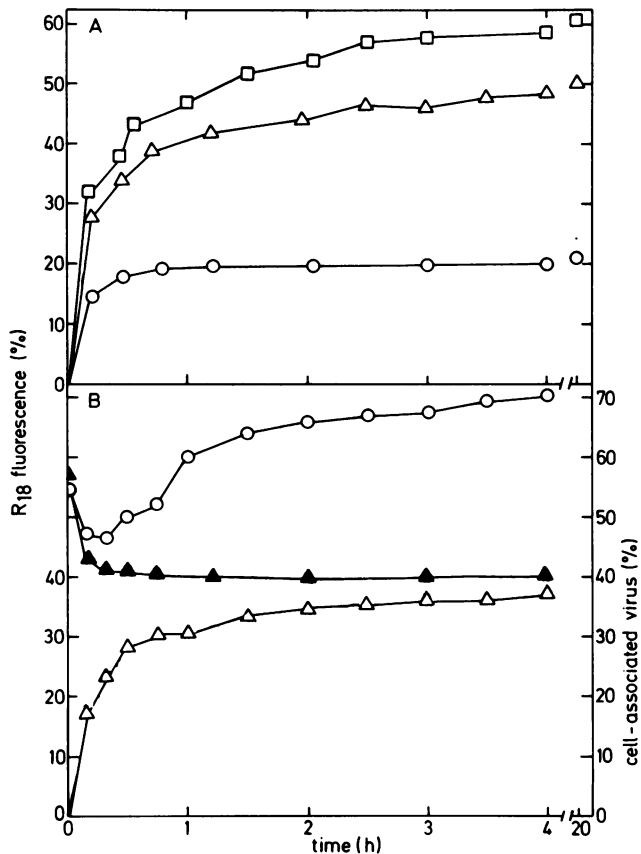
FIG. 7. Effect of removal of nonbound virus on the extent of fusion. (A) Virus (25 μg of protein) was incubated with various amounts of erythrocyte ghosts (50 [O], 100 [△], and 150 [□] μg of protein) for 15 min at 4°C. The final incubation volume was 0.4 ml. Nonbound virus was subsequently removed, the cells were washed once and resuspended in 2 ml of prewarmed buffer (37°C), and fusion was monitored as a function of time. The fluorescence scale in these experiments was calibrated by setting the cell-associated fluorescence at time zero (i.e., after the preincubation at 4°C and after removal of nonbound particles) at the zero level of the chart recorder (0% fusion) and the value obtained after the addition of Triton X-100, corrected for dilution, at 100% (100% fusion). (B) Virus (263 μg) and 750 μg of ghosts were mixed in 3 ml of buffer (final volume). The mixture was incubated at 4°C. After 15 min, the suspension was transferred, without removal of nonbound particles, to 37°C, and after various times 200-μl samples were taken, mixed with 800 μl of ice-cold buffer, and subsequently centrifuged. The cells were washed once. Fluorescence in the pellet fractions and the combined supernatants was measured before and after the addition of Triton X-100 (1% [vol/vol]). The percentage of cell-associated virus (O) and fusion (△) was determined as described in the text. The curve (▲) illustrates the kinetics of cell-associated virus release after preincubation of 25 μg of virus with 100 μg of ghosts for 15 min at 4°C, followed by the removal of nonbound virus, before the initiation of fusion at 37°C (see the legend to panel A).

which was observed when nonbound virions had been removed before the initiation of fusion (cf. O and ▲, Fig. 7B). Interestingly, in the presence of nonbound virus particles, the cell-associated fraction increased again after approximately 25 min when most of the initially cell-associated virus fraction had fused.

The nonbound virions and those released during incubation at 37°C do not represent an inactive virus fraction. Upon their removal and subsequent incubation with (fresh) ghosts, they bound and fused as avidly as a similar concentration of

the stock virus (data not shown). Yet it appears that the newly bound virions did not substantially raise the level of fusion (Fig. 7B; see Discussion). These results suggest that the initially bound virus fraction determines predominantly the course of fusion. Further experimental support for this suggestion was obtained from competition experiments with nonlabeled virions.

Competition between R_{18}-labeled and nonlabeled viruses. The degree of viral binding varied during the course of virus-target membrane interaction, depending on whether nonbound virus was removed after preincubation (Fig. 7). To examine the degree to which fusion was affected by these alterations in binding, we determined the extent to which nonlabeled virus could interfere with the fusion kinetics of R_{18}-labeled virus. In a typical experiment, 25 μg of R_{18}-labeled virus was added to 80 μg of ghosts at 37°C. The initial fusion rate was 2.76%/min. Alternatively, when the ghosts were pretreated with a sevenfold excess of nonlabeled virus at 4°C for 15 min, followed by the removal of nonbound virus, a residual fusion rate of 0.55%/min was obtained. Hence, prior treatment with nonlabeled virus resulted in an 80% inhibition of fusion. The efficiency of competition observed in the latter case appeared to be dependent on the incubation time at 37°C of the pretreated cells, prior to the addition of R_{18}-labeled virus. With addition after 30 s, inhibition was approximately 60%, whereas inhibition of 80% was obtained when the labeled virus was included in the medium after 2 min. Incubation times up to 90 min, prior to the addition of labeled virus, did not further increase the efficiency of inhibition. Finally, we examined the effect of adding the nonlabeled virus during the course of fusion between R_{18}-labeled virus and erythrocyte membranes. To this end, the labeled virus was preincubated with the ghosts for 15 min at 4°C. Nonbound virus was removed, and fusion was initiated by transferring the mixture to 37°C. After 2 min, various amounts of nonlabeled virus were injected into the medium. Relative to the fusion kinetics observed for the control (in the absence of nonlabeled virus), the kinetics in the presence of the nonlabeled virus particles were not affected (data not shown), even when the amount of nonlabeled virus was increased up to 400 μg of protein.

Dependence of Sendai virus-erythrocyte membrane interaction on the structural integrity of viral proteins. The biological activity of Sendai virus depends on the structural integrity of both the HN and F proteins (2, 4, 29). To gain insight into the relevance of intra- or intermolecular disulfide bonding for the proper functioning of the F and HN proteins, Sendai virus was pretreated with various concentrations of DTT (22, 28) and subsequently incubated with erythrocyte ghosts. The extent of fusion and binding was determined after 10 min of incubation. In addition, DTT-treated virus was incubated with (intact) human erythrocytes, and the extent of hemolysis was determined similarly. Fusion of the virus with ghosts and virus-induced hemolysis were inhibited to similar degrees (Fig. 8), the inhibiting effect already becoming apparent at a DTT concentration as low as 0.01 mM. The binding of the virus, i.e., the HN protein, appeared to be less affected. Under conditions in which fusion and hemolysis were inhibited by approximately 80% (0.5 mM DTT), substantial binding was still observed, i.e., approximately 70% of the fraction that would bind in the case of nontreated virus.

DISCUSSION

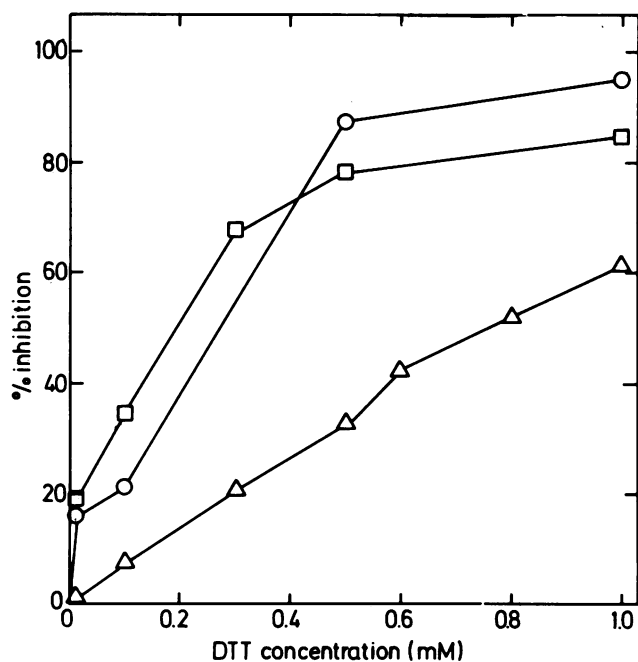Sendai virus binding. Sendai virus binds to erythrocyte membranes in a temperature-independent manner (Fig. 1),

FIG. 8. Effect of DTT on binding, fusion, and hemolysis activities of Sendai virus. Virus protein (60 μg) was treated with DTT at the final concentrations indicated for 15 min at 37°C in 0.15 ml of KNP buffer, as described in Materials and Methods. A control sample was treated similarly in the absence of the reducing agent. After treatment, the virus was injected into a cuvette containing 100 μg of ghosts in KNP buffer, and fusion was monitored continuously in a fluorometer. The extent of fusion, relative to the extent reached by a nontreated sample, was determined after 10 min. The percentage of inhibition was calculated and plotted as a function of DTT concentration (□). The effect on binding was determined by incubating the DTT-treated viruses with ghosts at 4°C for 10 min. Nonbound virus was removed by centrifugation, and after the cells were washed once more, cell-associated fluorescence was determined after the addition of Triton X-100 and compared with that of a nontreated sample (△). Virus-induced hemolysis was performed as described in Materials and Methods. The incubation conditions were such that the amount of R_{18}-labeled virus per number of erythrocytes per unit of volume (30 μg of virus per 1.8×10^8 cells per 2 ml) corresponded to the incubation conditions of the fusion experiments. The extent of hemolysis, relative to that induced by nontreated virus, was determined after 10 min and expressed as the percentage of inhibition versus the DTT concentration (○).

consistent with observations reported by others (2). The fraction of the viral dose which was bound was dependent on the target membrane concentration (Fig. 2), i.e., when the number of receptor sites increased, the fraction of bound virions increased. A maximal binding capacity of 700 to 1,750 virus particles was calculated (Fig. 2), yielding an average of ca. 1,200 Sendai virions per erythrocyte ghost. A similar value has been reported for the binding capacity of protein-labeled Sendai virus with intact erythrocytes (38), which adds to the reliability of the assay used in this work.

Relative to the binding kinetics at 4°C, the initial binding rate was slightly faster at 37°C (Fig. 1). An increase in the binding rate was also seen when the target membrane concentration was increased at a constant virus concentration (data not shown), culminating in an increase in the initial fusion rate (Fig. 4A). These observations are in line with an increase in the collision frequency between the particles, occurring under both conditions. An analysis of the virus-

ghost interaction process in terms of a mass-action kinetic model (25), which views the interaction as a sequence of the second-order process of virus-cell adhesion followed by the first-order fusion reaction itself, revealed a rate constant of adhesion of (1.9 to 3.5) × 10^9 M^{-1} s^{-1} (S. Nir and D. Hoekstra, unpublished observation). These values are close to those in diffusion-controlled processes.

Dissociation of target membrane-bound virus. A fraction of the cell-associated virus particles, recognized as firmly bound virus at 4°C, readily dissociated from the cell surface when the temperature was raised to 37°C. The release was independent of the presence of nonbound virus particles when left in the medium after preincubation (Fig. 7B). A variety of reasons argue against the involvement of neuraminidase activity in the elution process. First, in the presence of the neuraminidase inhibitor 2-deoxy-2,3-dehydro-N-acetylneuraminic acid (23), the extent of viral elution was unaffected at 4°C, whereas at 37°C 25% of the cell-associated virus still dissociated from the cell surface (versus 30% in the absence of inhibitor). Second, taking into account the multidentate binding character of the virus and comparing the kinetics of viral release with those of glycophorin desialylation (27, 34), the release was too fast to have been due to viral neuraminidase activity. Third, the experimental conditions described in this work are far from being favorable for optimal neuraminidase activity: (i) the medium contained a high concentration of Cl^- (150 mM), which strongly inhibits its activity (24), and (ii) during incubation the medium pH was 7.4, whereas the pH optimum of the enzyme is centered around pH 5.5 (24). Thus, rather than attributing it to viral neuraminidase activity, we attributed this dissociation process to an increase in the incubation temperature per se and, to a lesser extent, to dilution of the virus-cell complex after preincubation at 4°C (as approximately 5% of the cell-associated fraction was released upon resuspension in the 4°C medium). Both these processes are known to cause an increase in the dissociation rate constant (25), and by applying a mass-action kinetic model we estimated that in the case of virus-erythrocyte ghost interaction, the dissociation rate constant increased approximately 30-fold when the temperature was raised from 4 to 37°C (Nir and Hoekstra, unpublished observation). Based on the arguments described above, it remains to be seen to what extent desialylation is correlated to the release of virions, particularly in light of the multivalent binding character of the virus and the possibility that sialic acid forms only a part of the active binding site in the receptor (3).

Sendai virus fusion. The rate of Sendai virus fusion with the erythrocyte membrane was affected by the density of the virus particles on the cell surface and became relatively suppressed when more than 170 virus particles were attached per ghost (Fig. 5 and 6). This number is substantially lower than the maximal virus binding capacity (ca. 1,200; see above). Hence, it is assumed that fusion takes place in restricted areas, relatively densely populated with adhered viruses, rather than at random sites distributed over the entire cell surface. Support for this assumption is provided by observations that virus binding induces changes in the lateral distribution of cell membrane receptors by causing the formation of virus receptor patches in the plane of the plasma membrane (1, 21). Moreover, examination of ghosts incubated with fluorescently labeled virus (10, 12) revealed the presence of numerous fluorescent spots at the cell periphery after low-temperature preincubation, rather than a uniform ring of attached virions. This indicates that the subsequent fusion event, which occurred when the temper-

ature was raised to 37°C, takes place at densely populated sites on the cell surface, the net density being dependent on the attached multiplicity, which, in turn, depends on the input multiplicity (Fig. 2).

An interesting and intriguing outcome of this study was the finding that although ca. 1,200 viruses can bind per cell, only some 180 particles maximally can fuse. It should be noted that all virus particles added to the cells possess fusion activity (see below). Hence, in line with the discussion in the previous paragraph, these results further indicate that a limited number of fusion-susceptible sites exist on the cell surface at which the binding of the virus eventually leads to fusion. Whether specific molecular properties can be attributed to these sites remains to be elucidated. The presence of specific fusion sites on the cell surface for paramyxoviruses has been suggested before (30). It is possible that other factors contribute as well to a limited fusion capacity of viruses per ghost. Alterations of membrane fluidity owing to virus-induced cross-linking of cell membrane receptors (1, 19, 21) and the rate of viral protein diffusion (2, 18) from the fusion areas may additionally affect the fusion ability of viral particles which are about to fuse, particularly during the early stages of the fusion process. However, both these possibilities do not mutually exclude the existence of specific fusion sites on the ghost surface.

An important consequence of a limited fusion capacity per erythrocyte ghost is that at high virus-to-ghost ratios binding is favored relative to the cell-associated fraction which actually fuses (Fig. 5). Hence, to obtain the highest fusion efficiency possible, it is desirable to keep the attached multiplicity below ca. 180 virus particles per ghost. From the data shown in Fig. 2 and 4A it can be calculated that when this requirement is met, most of the cell-associated virus fuses. For example, with 40 µg of ghosts, some 130 to 140 virus particles become attached per ghost; the final level of fluorescence indicated that ca. 120 virions fused per ghost. The experiments described in Fig. 4A also indicated that the limited fusion capacity is determined by the ghost and not by the virus. At the lowest input multiplicity (15 µg of virus per 160 µg of ghosts), virtually all virus particles added to the cell suspension eventually fused, i.e., essentially all viral particles can, in principle, display fusion activity. Finally, the results shown in Fig. 7A also support the conclusion that at a relatively low attached multiplicity, nearly all cell-associated virus fuses. Taking into account that a fraction of the initially cell-associated virus dissociates from the cell surface when the virus-ghost complex is transferred to 37°C, it can be calculated that at the highest ghost concentrations (100 and 150 µg) more than 80% of the cell-associated virions fused with the target membrane.

Despite the release of a significant fraction of preattached virions when fusion was initiated at 37°C and the increase in viral attachment at later stages (Fig. 7B), the kinetics of fusion proceeded very smoothly (Fig. 3 and 7B). This indicated that the loosely bound fraction of virions does not substantially affect the course of fusion per se, nor does the fraction which subsequently became cell associated. In fact, under the conditions described in Fig. 7B, it was calculated that ca. 70% of the initially bound virions fused after 25 min. Assuming that, in time, the total fraction fuses, fusion of ca. 10% of the newly bound virions is required to account for the maximal fusion level reached (Fig. 4B). On the other hand, if the ability of the initially bound virions to fuse abruptly halted after 25 min (Fig. 7B), which seems very unlikely, an upper limit of ca. 40% of the newly bound virions should fuse to reach the fusion maximum. Thus, it appears that the

course and extent of fusion were determined mainly by the virus fraction which remained firmly cell associated after the temperature was raised to 37°C. Moreover, the competition experiments between R_{18}-labeled and nonlabeled virus indicated that during the early stages of virus-target membrane interaction a fraction of the virus attaches rapidly to binding sites which render the virus susceptible to fusion in an overall irreversible manner, i.e., once the particles attach to these sites they bind irreversibly, and eventually they fuse. This can be inferred from the observation that only pretreatment of the ghosts with unlabeled virions effectively inhibited the fusion of labeled ones.

Role of viral proteins. The observation that treatment of the virus with DTT substantially reduced viral binding (Fig. 8) suggests that the interaction between the HN protein and the sialic acid residues of glycophorin is not purely an electrostatic interaction (2). Because more than 90% of the HN protein exists in disulfide-linked dimeric and tetrameric forms (22), the results imply that structural requirements have to be met as well for the protein to interact properly with the receptor. Such requirements could involve, for example, dependence of binding on the conformation of the HN protein or the need for the establishment of multivalent interactions for stable virion binding between a receptor molecule and a di- or tetrameric HN protein molecule or both.

Finally, the dependence of viral fusion activity on a structurally intact F protein was also readily revealed by the present experimental approach. The results indicate that a subtle perturbation (28) of the F protein structure suffices to completely perturb its functional activity. This emphasizes the strong dependence of the virus on the conformation of the F protein to express its biological activity.

ACKNOWLEDGMENTS

LITERATURE CITED

1. **Altstiel, L. D., and F. R. Landsberger.** 1981. Structural changes in BHK cell plasma membrane caused by the binding of vesicular stomatitis virus. J. Virol. **39:**82–86.
2. **Bächi, T., J. E. Daes, and C. Howe.** 1977. Virus-erythrocyte membrane interactions, p. 83–127. *In* G. Poste and G. L. Nicholson (ed.), Virus infection and the cell surface. Elsevier Biomedical Press, Amsterdam.
3. **Burness, A. T., and I. U. Pardoe.** 1983. A sialoglycopeptide from human erythrocytes with receptor-like properties for encephalomyocarditis and influenza viruses. J. Gen. Virol. **64:**1137–1148.
4. **Choppin, P. W., C. D. Richardson, D. C. Merz, W. W. Hall, and A. Scheid.** 1981. The functions and inhibition of the membrane glycoproteins of paramyxoviruses and myxoviruses and the role of the measles virus M protein in subacute sclerosing panencephalitis. J. Infect. Dis. **143:**352–363.
5. **Cohen, C. M., and A. K. Solomon.** 1976. Ca binding to the human red cell membrane: characterization of membrane preparations and binding sites. J. Membr. Biol. **29:**345–372.
6. **Fries, E., and A. Helenius.** 1979. Binding of Semliki Forest virus and its spike glycoproteins to cells. Eur. J. Biochem. **97:**213–220.
7. **Gething, M. J., J. M. White, and M. D. Waterfield.** 1978. Purification of the fusion protein of Sendai virus: analysis of the NH_2-terminal sequence generated during precursor activation.

Proc. Natl. Acad. Sci. USA **75:**2737–2740.

8. **Haywood, A. M.** 1974. Fusion of Sendai virus with model membranes. J. Mol. Biol. **87:**625–628.

9. **Haywood, A. M., and B. P. Boyer.** 1982. Sendai virus membrane fusion: time course and effect of temperature, pH, calcium and receptor concentration. Biochemistry **21:**6041–6046.

10. **Henis, Y. I., and T. M. Jenkins.** 1983. Detection of Sendai virus fusion with human erythrocytes by fluorescence photobleaching recovery. FEBS Lett. **151:**134–138.

11. **Hoekstra, D., T. de Boer, K. Klappe, and J. Wilschut.** 1984. Fluorescence method for measuring the kinetics of fusion between biological membranes. Biochemistry. **23:**5675–5681.

12. **Hoekstra, D., K. Klappe, T. de Boer, and J. Wilschut.** 1985. Characterization of the fusogenic properties of Sendai virus: kinetics of fusion with erythrocyte membranes. Biochemistry **24:**4739–4746.

13. **Hoekstra, D., J. Wilschut, and G. Scherphof.** 1985. Calcium phosphate-induced fusion of erythrocyte ghosts; kinetic characterization and the role of Ca^{2+}, phosphate and calcium-phosphate complexes. Eur. J. Biochem. **146:**131–140.

14. **Holmgren, J., L. Svennerholm, H. Elwing, P. Fredman, and O. Strannegaro.** 1980. Sendai virus receptor: proposed recognition structure binding to plastic-adsorbed gangliosides. Proc. Natl. Acad. Sci. USA **77:**1947–1950.

15. **Hsu, M.-C., A. Scheid, and P. W. Choppin.** 1981. Activation of the Sendai virus fusion protein (F) involves a conformational change with exposure of a new hydrophobic region. J. Biol. Chem. **256:**3557–3563.

16. **Klenk, H.-D., and P. W. Choppin.** 1969. Chemical composition of parainfluenza virus SV 5. Virology **37:**155–157.

17. **Lenard, J., and D. K. Miller.** 1983. Entry of enveloped viruses into cells, p. 121–138. *In* P. Cuatrecasas and T. Roth (ed.), Receptor-mediated endocytosis and processing. Chapman & Hall Ltd., London.

18. **Loyter, A., and D. J. Volsky.** 1982. Reconstituted Sendai virus envelopes as carriers for the introduction of biological material into animal cells. Cell Surf. Rev. **8:**215–266.

19. **Lyles, D. S., and F. S. Landsberger.** 1979. Kinetics of Sendai virus envelope fusion with erythrocyte membranes and virus-induced hemolysis. Biochemistry **18:**5088–5095.

20. **Maeda, T., A. Asano, Y. Ohki, Y. Okada, and S. Ohnishi.** 1975. A spin-label study on fusion of red blood cells induced by hemagglutinating virus of Japan. Biochemistry **14:**3736–3741.

21. **Maeda, T., C. Eldridge, S. Toyama, S.-I. Ohnishi, E. L. Elson, and W. W. Webb.** 1979. Membrane receptor mobility changes by Sendai virus. Exp. Cell Res. **123:**333–343.

22. **Markwell, M. A. K., and C. F. Fox.** 1980. Protein-protein interactions within paramyxoviruses identified by native disulfide bonding or reversible chemical cross-linking. J. Virol. **33:**152–166.

23. **Meindl, P., G. Bodo, P. Palese, J. Schulman, and H. Tuppy.** 1974. Inhibition of neuraminidase activity by derivatives of 2-deoxy-2,3-dehydro-*N*-acetyl neuraminic acid. Virology **58:**457–463.

24. **Merz, D. C., P. Prehm, S. Scheid, and P. W. Choppin.** 1981. Inhibition of the neuraminidase of paramyxoviruses by halide ions: a possible means of modulating the two activities of the HN protein. Virology **112:**296–305.

25. **Nir, S., J. Bentz, J. Wilschut, and N. Düzgünes.** 1983. Aggregation and fusion of phospholipid vesicles. Prog. Surf. Sci. **13:**1–124.

26. **Oku, N., K. Inoue, S. Nojima, T. Sekiya, and Y. Nozawa.** 1982. Electron microscopic study on the interaction of Sendai virus with liposomes containing glycophorin. Biochim. Biophys. Acta **691:**91–96.

27. **Oku, N., S. Nojima, and K. Inoue.** 1981. Studies on the interaction of Sendai virus with liposomal membranes. Sendai virus-induced agglutination of liposomes containing glycophorin. Biochim. Biophys. Acta **646:**36–42.

28. **Ozawa, M., A. Asano, and Y. Okada.** 1979. The presence and cleavage of interpeptide disulfide bonds in viral glycoproteins. J. Biochem. **86:**1361–1369.

29. **Poste, G., and C. Pasternak.** 1978. Virus-induced cell fusion. Cell Surf. Rev. **5:**305–367.

30. **Richardson, C. D., and P. W. Choppin.** 1983. Oligopeptides that specifically inhibit membrane fusion by paramyxoviruses: studies on the site of action. Virology **131:**518–532.

31. **Roux, L., and J. J. Holland.** 1979. Role of defective interfering particles of Sendai virus in persistent infections. Virology **93:**91–103.

32. **Tozawa, H., M. Watanabe, and A. Ishida.** 1973. Structural components of Sendai virus. Serological and physiochemical characterization of hemagglutinin subunit associated with neuraminidase activity. Virology **55:**242–253.

33. **Umeda, M., S. Nojima, and K. Inoue.** 1983. HVJ-mediated fusion between erythrocyte membranes and liposomes containing glycophorin. J. Biochem. **94:**1955–1966.

34. **Umeda, M., S. Nojima, and K. Inoue.** 1984. Activity of human erythrocyte gangliosides as a receptor to HVJ. Virology **133:**172–182.

35. **Van Meer, G., and K. Simons.** 1983. An efficient method for introducing defined lipids into the plasma membrane of mammalian cells. J. Cell Biol. **97:**1365–1374.

36. **White, J., M. Kielian, and A. Helenius.** 1983. Membrane fusion proteins of enveloped animal viruses. Q. Rev. Biophys. **16:**151–195.

37. **Wilschut, J., and D. Hoekstra.** 1984. Membrane fusion: from liposomes to biological membranes. Trends Biochem. Sci. **9:**479–483.

38. **Wolf, D., I. Kahan, S. Nir, and A. Loyter.** 1980. The interaction between Sendai virus and cell membranes. Exp. Cell Res. **130:**361–369.

39. **Wu, P.-S., R. W. Ledeen, S. Udem, and Y. A. Isaacson.** 1980. Nature of the Sendai virus receptor: glycoprotein versus ganglioside. J. Virol. **33:**304–310.

40. **Wunner, W. H., K. J. Reagan, and H. Koprowski.** 1984. Characterization of saturable binding sites for rabies virus. J. Virol. **50:**691–697.